Journal of Power Sources 195 (2010) 536–540

Contents lists available at ScienceDirect

Journal of Power Sources

journal homepage: www.elsevier.com/locate/jpowsour

Short communication

Water permeation analysis on gas diffusion layers of proton exchange membrane fuel cells for Teflon-coating annotation

Yen-I Chou[a,*], Zih-Yuan Siao[a,b], Yu-Feng Chen[a], Lung-Yu Sung[a], Wen-Mei Yang[b], Chi-Chuan Wang[a]

[a] Energy and Environment Research Laboratories, Industrial Technology Research Institute, Chutung 310, Taiwan
[b] Department of Mechanical Engineering, National Chiao Tung University, Hsinchu 300, Taiwan

ARTICLE INFO

Article history:
Received 23 July 2009
Accepted 29 July 2009
Available online 7 August 2009

Keywords:
Proton exchange membrane fuel cells
Gas diffusion layer
Hydrophobic
Water permeation
Water flooding
Polytetrafluoroethylene

ABSTRACT

This study presents an analysis of water permeation of a polytetrafluoroethylene (PTFE)-coated gas diffusion layer (GDL) to determine the influence of hydrophobic treatment on the GDL for diagnosis of water flooding. It is found that the behaviour of water drainage is controlled by the pore configuration instead of the hydrophobicity in GDL. Better water drainage is achieved by the action of the Teflon coating in modulating the GDL pore configuration to give both a larger average pore size and a wider distribution of pore size. The results show that water penetration through the GDL must overcome a threshold surface tension defined by the largest pore range. A 30 wt.% PTFE coating of a GDL is shown to generate a satisfactory pore configuration, explaining the improved cell polarization performance with a lower driven pressure (~1.91 kPa) and a higher rate of water drainage.

1. Introduction

The proton exchange membrane fuel cell (PEMFC) is one of the most promising energy resources for the future due to its advantages of high power density at low temperature, very low or zero emission of greenhouse gases, long-term reliable operation and facility of system set-up [1–3]. However, it is well known that PEMFC suffers from water flooding, commonly from the reaction at the cathode, $O_2 + 4H^+ + 4e^- \rightarrow 2H_2O$, especially during high power density operation [4,5]. The excess water accumulates in the membrane electrode assembly (MEA), which blocks the oxygen feed and deteriorates the cell polarization performance considerably. For efficient water management, the gas diffusion layer (GDL) is commonly hydrophobically treated with polytetrafluoroethylene (PTFE) for flooding mitigation. A Teflon coating on a GDL is intended to engender vapour diffusion and water shear force for efficient drainage [3,6–8]. Velayutham et al. [9] examined the effects of PTFE contents in the range 7–30 wt.% and found a 23 wt.% Teflon-coated GDL to be optimal in terms of flooding diagnosis. Tüber et al. [10] demonstrated that a 20 wt.% PTFE coating produces a strongly hydrophobic GDL, which leads to superior cell performance at room temperature. The review by Li et al. [3] showed an optimal concentration of PTFE within 20–40 wt.%, depending on the conditions used for the preparation of GDL samples. It is believed that the PTFE coating on a GDL is a compromise between pore hydrophobicity and pore configuration [11,12]. Normally, too little PTFE coating results in insufficient hydrophobicity for water removal, while excessive PTFE loading causes an inferior cell performance, since it blocks the GDL pore void and reduces electrical conductivity.

Direct observation of flooding into GDL is quite complicated and may interfere with both the GDL specimen and the operating conditions. Most studies have examined only the outcome of GDL hydrophobic treatment by cell polarization testing [12–15] or computational modelling [16,17]. However, these characterizations were usually accompanied by many other operative effects, which inevitably obscure the actual flooding phenomenon inside PEMFC systems. This could explain the lack of the direct evidence needed to specify the degree of PTFE coating for flooding diagnosis. Recently, Benziger et al. [18] described a pressurized membrane filtration system for simulating water penetration through a GDL in order to evaluate the role of the PTFE coating. Firstly, they found that the water must achieve a threshold pressure to force water through the largest pores in the GDL. Secondly, they showed the largest pores in a GDL were effective for drainage of water flooding. And the water drainage was dominated by only a small portion of void in GDL. This result implies the water drainage was correlated largely with the pore configuration of the GDL, which differs from the common viewpoint of hydrophobic promotion. The objective of this study was to extend the experiments with water-pressurized GDL filtration to a broader range of operative pressures, combined with an examination of the influence of pore configuration on water drainage for various PTFE-coated GDLs. Moreover, the effect of PTFE

* Corresponding author. Tel.: +886 3 5919277; fax: +886 3 5829782.
E-mail address: cecilchou@itri.org.tw (Y.-I. Chou).

0378-7753/$ – see front matter © 2009 Elsevier B.V. All rights reserved.
doi:10.1016/j.jpowsour.2009.07.049

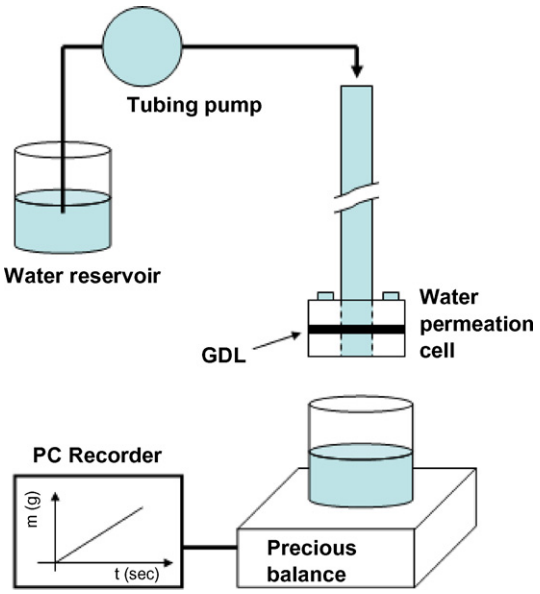

Fig. 1. A diagram of the pressurized water filtration system. The pressure is measured as the height of the hydrostatic head of the water above the GDL.

treatment on GDLs was examined with respect to modulation of adequate pore configuration instead of the surface hydrophobicity in GDL.

2. Experimental approach

2.1. Hydrophobic Teflon coating and characterization

The GDLs were all obtained from SIGRACET® GDL (SGL 10AA, SGL Carbon Group, Germany) as carbon papers without PTFE or microporous layer (MPL) coating. The carbon papers were cut into 2.4 cm × 2.4 cm squares and immersed in a PTFE aqueous dispersion solution (DuPont™ Teflon® PTFE TE-3893) for 30 min. PTFE emulsions of 15–60 wt.% were prepared. The coated carbon papers were air-dried at 120 °C for 1 h, and subsequently sintered in a furnace at 350 °C under a nitrogen atmosphere with a temperature rising rate of 3 °C min^{-1} for 30 min. The treated GDLs were characterized by optical microscopy (OM) (BX51, Olympus) and scanning electron microscopy (SEM) (JSM-7000F, JEOL) for surface morphological and structural observations, respectively. The hydrophobicity of the GDLs was characterized by the contact angle with a static water drop shape analysis system (DSA100, KRÜSS). The contact angle was determined as the average value of at least three measurements of 10 μL water droplets at randomly chosen regions on each GDL sample. The porous structure of the GDL was characterized with a mercury porosimeter (Autopore 9520, Micromeritics). The average pore size and size distribution were determined from the mercury intrusion by an applied pressure based on capillary law.

2.2. Water permeation characterization

The water permeation through GDL was characterized in a pressurized membrane filtration cell. As shown in Fig. 1, the GDL was placed on a laboratory-built polymethylmethacrylate (PMMA) cell attached to a 70 cm high, 1.4 cm diameter cylinder. Initially, a peristaltic pump (MP-1000, EYELA) was used to introduce water into the cylinder slowly (0.2 g min^{-1}) until the water started to penetrate the GDL. When the water started to drain out of the GDL, the hydrostatic head, i.e. the height of the water in the cylinder, was recorded as the threshold pressure P_{th}. The pump was regulated to maintain P_{th} in order to measure the drained water flow. The amount of water drainage was recorded with a precision balance (GF-300, A&D) with a time interval of 5 s. The water permeation behaviour at pressures >P_{th}, i.e. higher hydrostatic heads, was characterized. Unlike the study reported by Benziger et al. [18], the water permeation characteristics and its influence subject to pore structure variation were examined above the threshold pressure.

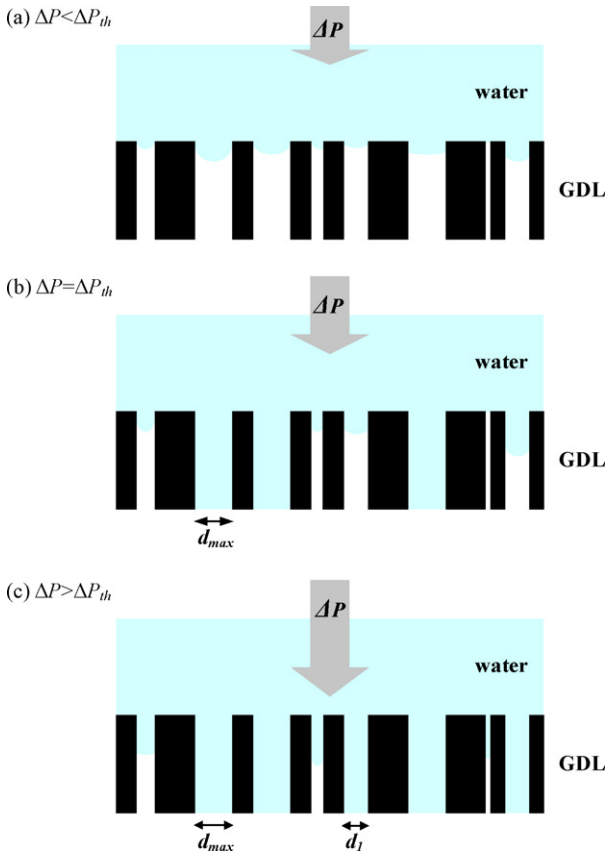

Fig. 2. A model of the pressurized water penetration through the GDL with transverse cylindrical pairs of different diameters under (a) $P < P_{th}$, (b) $P = P_{th}$, and (c) $P > P_{th}$.

3. Water permeation analysis

Fig. 2 shows a diagram for water penetration through the GDL with various pore diameters under different driven pressures. In this model, it is assumed that the pores are cylindrical and distributed non-uniformly. The penetration pressure ΔP of water into a pore of size d in GDL can be described by the Young and Laplace relation [19]:

$$\Delta P = \frac{4\gamma \cos\theta}{d} \quad (1)$$

where γ is the surface tension of water, θ is the contact angle of water with the pore surface, and d is the pore diameter. As shown, the water is first expelled from the pores when the applied pressure is insufficient to override the surface tension (as shown in the case of $\Delta P < \Delta P_{th}$ in Fig. 2(a)). When the pressure is increased to ΔP_{th}, the water can overcome the minimum surface tension and start to penetrate through the GDL via the largest pores (d_{max}) as shown in Fig. 2(b). With this micro-sized pore configuration, a laminar flow should prevail through these pores, hence the water flow rate (Q_{th}) drained from d_{max} can be described by Darcy's law [20]:

$$Q_{th} = K_{th}\Delta P_{th} = \frac{k_{th}A_{th}}{\mu L}\Delta P_{th} \quad (2)$$

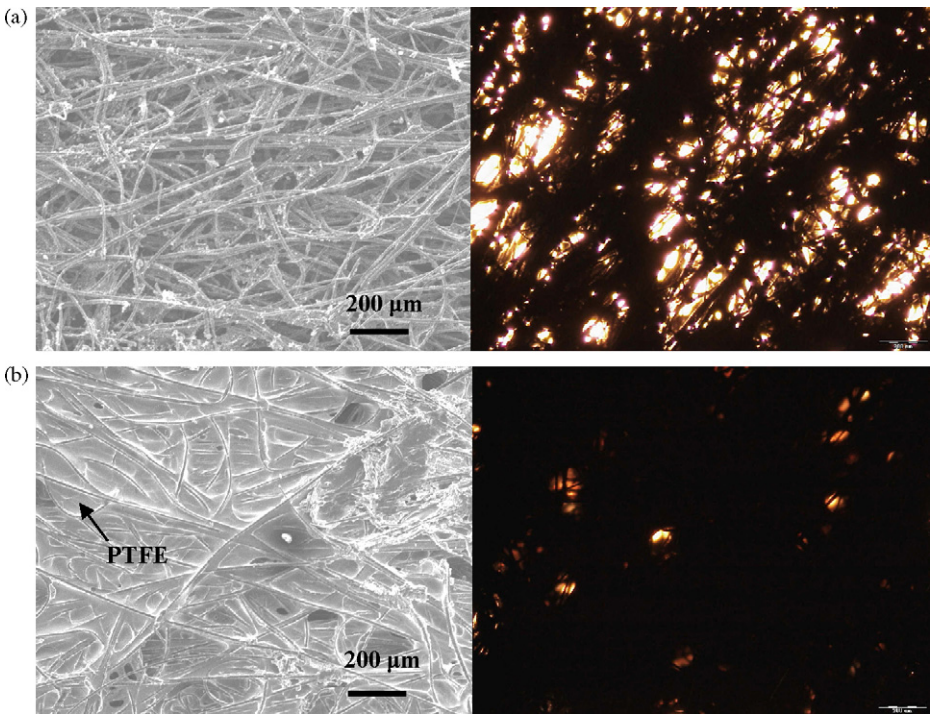

Fig. 3. SEM and OM images of (a) the uncoated and (b) the 100 wt.% Teflon-coated GDLs.

where k_{th} is the intrinsic permeability coefficient of water at pore d_{max}, A_{th} is the total area of d_{max} pores, μ is the viscosity of water, and L is the penetration length of water at a GDL thickness of 0.38 mm. As shown in Fig. 2(c), a further increase of the pressure to ΔP_1 (when $\Delta P > \Delta P_{th}$) is applied for water penetration to overcome the higher resistance from pores of small diameter (d_1). In this respect, the flow rate (Q_1) at ΔP_1 is related to the water fluxes from pores d_{max} and d_1:

$$Q_1 = K_1 \Delta P_1 = K_{th} \Delta P_1 + K_1' \Delta P_1 \quad (3)$$

where K_1 is the apparent permeability of water at ΔP_1 through d_{max} and d_1, and K_1' is the permeability of water through only d_1.

With a further rise of applied pressure to ΔP_n, the pore sizes larger than d_n are all activated for water penetration. Thus, K_n for all penetrable pore sizes (from d_n to d_{max}) and the K_n for pore d_n are:

$$K_n = \frac{Q_n}{\Delta P_n} \quad (4)$$

$$K_n' = K_n - K_{th} - \sum_{i=1}^{n-1} K_i = \frac{k_n A_n}{\mu L} \quad (5)$$

where A_n is the total penetration area for pore size d_n. Here, the flow rate q_n for the indicated pores d_n can be obtained from $\pi \Delta P_n d_n^4 / 128 \mu L$ and subsequently A_n can be evaluated from $n_n \pi (d_n/2)^2$, where the pore number (n_n) is determined by $(Q_n - K_{n-1} \Delta P_n)/q_n$. Once A_n is known, the permeability coefficient of k_n for pore size d_n can be obtained from Eq. (5). According to this analysis, the behaviour of water penetration and the pore configuration of GDL are correlated. It can be seen from the results presented above that drainage in the fuel cell is dominated by macropores; therefore, the water-pressurized GDL filtration in this work was characterized at hydrostatic heads of <70 cm, which focuses on pores with a diameter >30 μm. This study was designed to characterize water penetration behaviour with pressure-activated pore structure in order to explain the benefit of the Teflon coating for GDL.

4. Results and discussion

Fig. 3 shows typical SEM and OM images of GDLs with and without a PTFE coating. It is clear that the PTFE is coated on the cross space of the carbon fibres. The PTFE coating reduces the void volume and the pore number of the GDL. Fig. 4 shows the pore distribution of GDLs with different PTFE loadings. The majority of pore sizes of the GDLs were in the range 20–400 μm (macropores) with a few in the range 0.2–10 μm (micropores). For the uncoated GDL, the porosity ϕ is 91.0% and the average pore diameter d_{av} is 61.4 μm. With the PTFE coating, the voids in both micro- and macro-regions are inevitably reduced. This is especially conspicu-

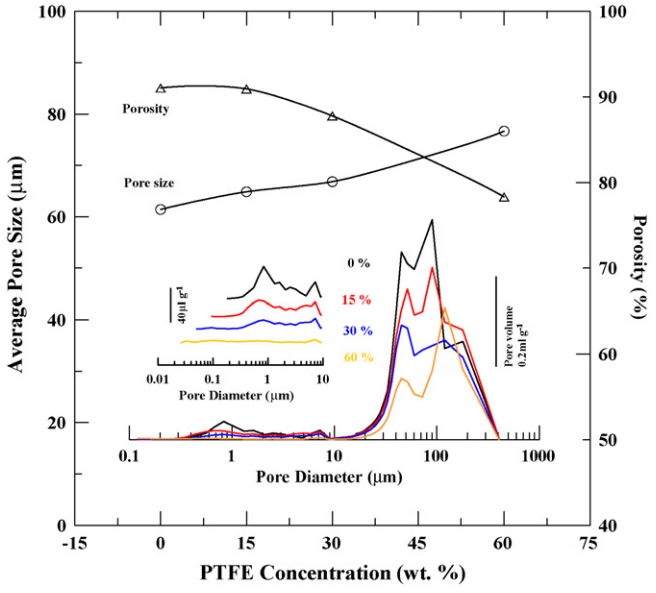

Fig. 4. Average pore size and porosity of GDLs with different PTFE coatings. Inset: pore size distribution of Teflon-coated GDLs.

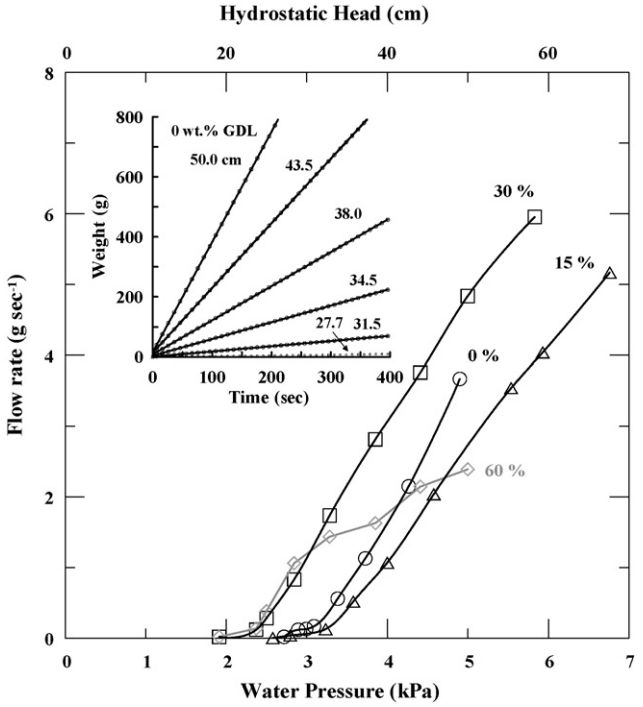

Fig. 5. Effect of hydrostatic pressure on the water flow rate for various Teflon-coated GDLs. Inset: time-dependent water weight drained from uncoated GDL at various hydrostatic pressures.

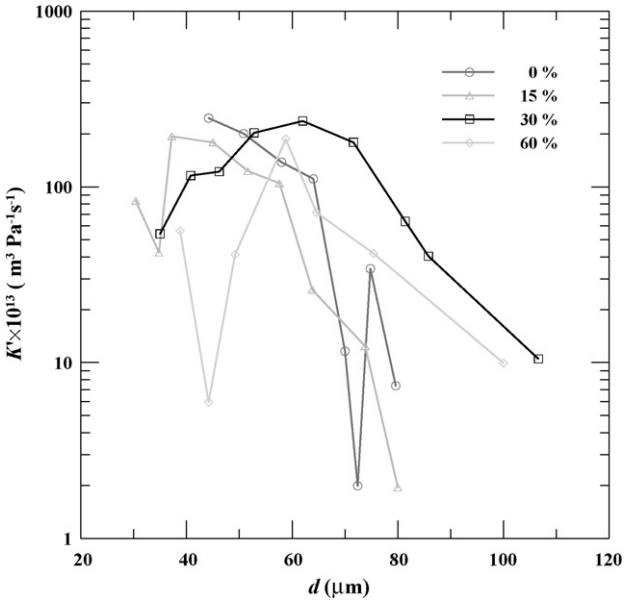

Fig. 6. Plots of K' *versus* d for various Teflon-coated GDLs.

ous for small pores, where the Teflon fills a considerable portion of voids, smoothing out the micropore region and leading to a larger average pore size. It is shown that the porosity is reduced to 78.3% but the average pore size is increased to 76.7 μm for a PTFE concentration of 60 wt.%.

Fig. 5 illustrates the flow rates of different PTFE-coated GDLs under various hydrostatic head heights and the inset shows the weight of water drained from the GDL. The linearity of water drained *versus* time indicates these flow rates are constant and stable for the relevant pore structure regime. Fig. 5 shows that, due to the hydrophobicity of GDL, no water drainage can be achieved when the height of the hydrostatic head is lower than that corresponding to the penetration pressure ΔP_{th}. These ΔP_{th} values are 2.72 kPa (27.7 cm), 2.58 kPa (26.3 cm), 1.91 kPa (19.5 cm), and 2.02 kPa (20.6 cm) for 0 wt.%, 15 wt.%, 30 wt.%, and 60 wt.% PTFE-coated GDLs, respectively. According to Eq. (1), the maximum pore diameter for each P_{th} value corresponds to 67.7 μm, 84.4 μm, 117.6 μm, and 113.7 μm for 0 wt.%, 15 wt.%, 30 wt.%, and 60 wt.% PTFE-coated GDLs, respectively. This result coincides with the pore analysis from mercury-intrusion porosimetry, which showed that the maximum pore size increased with increased concentration of PTFE. With more PTFE coating, the voids in the micropores are further filled, thereby enhancing the wt.% of macropores and resulting in a decrease of ΔP_{th} for the initial draining. These characteristics of GDLs with different amounts of PTFE coating are summarized in Table 1.

Table 1
Characteristics of GDLs coated with various PTFE emulsion concentrations.

PTFE(%)	ΔP_{min} (Pa)	θ (°)	d_{avg} (μm)	d_{max}[a] (μm)	ϕ (%)
0	2716.6	129.7	61.4	67.7	91.0
15	2577.4	139.1	64.8	84.4	90.9
30	1911.0	141.3	66.0	117.6	87.8
60	2018.8	142.9	76.7	113.7	78.3

[a] d_{max} is calculated based on γ of 71.975 mN m^{-1} at 298 K from Eq. (1) [21].

Also shown in Fig. 5, the 30 wt.% PTFE-coated GDL exhibits the superior water penetration with its lower P_{th} and higher flow rates. This result is compatible with those of other studies, where the concentration of PTFE emulsion was 20–40 wt.% [22] for attainable water drainage and polarization performance. Besides, it is noted that the flow rate is not in linear proportion to the driving pressure, which implicates a discrepancy in Darcy's law. Part of the explanation might be that the GDL has an uneven distribution of pore size and a tortuous pore structure, showing a departure from Darcy's assumption of single cylindrical pore distribution. The K' values of GDLs at various pore diameters in Fig. 6 indicate that 30 wt.% GDL has the desired K' characteristics applicable to a large pore range of 60–110 μm. The uncoated GDL also shows acceptable water drainage, but it is limited to pores <65 μm. It can be seen from Eq. (5) that the K' for each range of pore size is controlled by two parameters; i.e. intrinsic permeability, k, and permeance area, A. The k property is independent of flowing fluid, but is often correlated with the configuration of porous media via the well known formula as $k = cd^2$ where c is a dimensionless constant for pore structural properties. A can be identified from the quantity of the indicated pore size and further related to the pore configuration of the GDL.

Fig. 7 shows the k values evaluated from various Teflon-coated GDLs with different pore diameters. Most k values are $<2.0 \times 10^{-10}$ m^2 and are proportional to d^2 with a slope of 0.031 ($c \sim 1/32$), which is in good agreement with Poiseuille's law:

$$Q = \frac{1}{32}\frac{d^2 A}{\mu L}\Delta P \tag{6}$$

The inset in Fig. 7 shows the pore size distributions of different Teflon-coated GDLs can be obtained from this water penetration analysis. For an uncoated GDL, the small pore size range controls water drainage. With Teflon coating, the effective pore size of GDL shifts to a larger pore size range and the 30 wt.% Teflon-coated GDL provides the largest average pore size of 40–120 μm and the widest pore size distribution for superior water drainage with lower threshold pressures as well as efficient drainage flux. It is well known that a Teflon coating raises the GDL hydrophobicity and minimizes vapour condensation. However, the variation of pore configuration along with the Teflon coating can lead to significant improvement of water drainage. This manipulation of GDL pore dis-

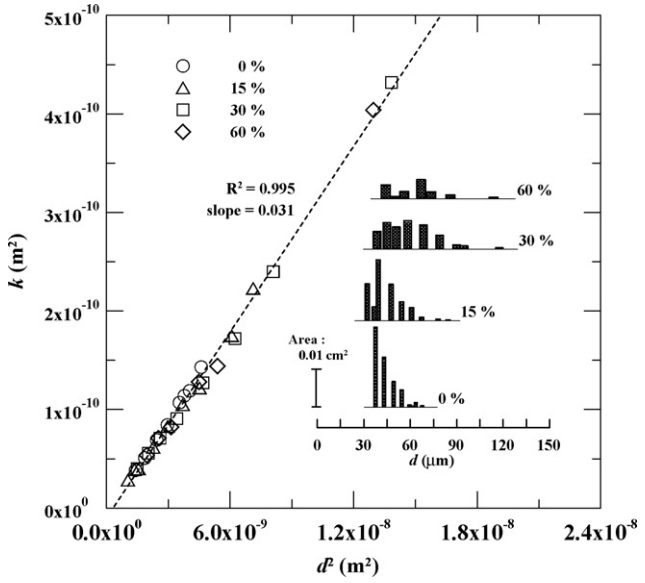

Fig. 7. Linear plot of k *versus* d^2 for various Teflon-coated GDLs. Inset: macropore size distribution of the Teflon-coated GDLs.

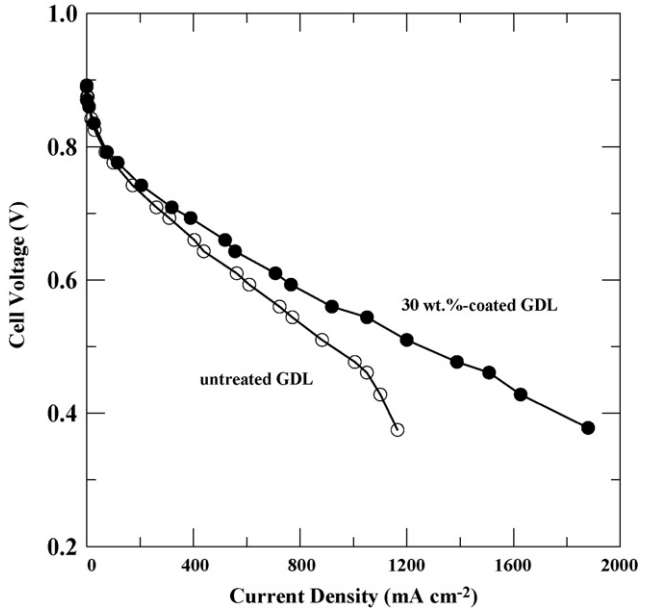

Fig. 8. The polarization curves of PEM fuel cells with uncoated and 30 wt.% Teflon-coated GDLs.

tribution gives rise to an effective increase of macropores, assisting the water drainage at a smaller ΔP_{th} and a higher flux performance. For further verification of the results, polarization tests were done for evaluation of the Teflon coating. Voltage-controlled measurements were performed with a Gore PRIMEA® 5621using anode and cathode catalyst loadings of 0.45 (Pt-Ru) and 0.6 (Pt) mg cm^{-2} at a cell temperature of 65 °C and at an ambient pressure of 1 atm. From two serpentine flow field channels, anode and cathode gases were fed with 1.5× and 3.0× H_2/air stoichiometries at 70 °C and 80 °C humidification, respectively. Fig. 8 shows the polarization difference between Teflon-coated and uncoated GDLs. From a current density of 400 mA cm^{-2}, the cell voltage of the uncoated GDL was lower than that of a 30 wt.% Teflon-coated GDL by approximately 5% and the difference was increased with a further increase of current density. When the current density exceeded 1000 mA cm^{-2}, there was a further substantial drop of cell voltage for the untreated GDL due to considerable water flooding. In summary, with an appropriate Teflon coating to modulate the pore configuration on the GDL, it is possible to achieve adequate water management for superior cell polarization performance.

5. Conclusions

The results of a water permeation analysis of various PTFE-coated GDLs are presented in this study. It was shown that the pore configuration of a GDL has a key role in the diagnosis of water flooding. In line with the proposed water penetration mechanism, water drainage began from the largest pores in a GDL, and the intrinsic water permeability of a GDL was controlled by pore size only. The effect of a PTFE coating on the pore configuration is important, since it provides a dramatic improvement of water drainage from a GDL. The contribution of the pore configuration to drainage outweighs the influence of hydrophobicity. In this work, the experimental results showed that a 30 wt.% PTFE-coated GDL had larger macropores, which resulted in superior cell polarization performance featuring a favourable water drainage characteristic and a greater permeability efficiency at a much lower driven pressure.

Acknowledgements

Part of this work is financially supported by the Department of Industrial Technology, Ministry of Economic Affairs, Taiwan. Authors wish to express their thanks to Dr. Huan-Ruei Shiu for his help in GDL support and technique discussion.

References

[1] B.C.H. Steele, A. Heinzel, Nature 414 (2001) 345–352.
[2] F. Barbir, PEM Fuel Cells, Elsevier Academic Press, Burlington, 2005.
[3] H. Li, Y. Tang, Z. Wang, Z. Shi, S. Wu, D. Song, J. Zhang, K. Fatih, J. Zhang, H. Wang, Z. Liu, R. Abouatallah, A. Mazza, J. Power Sources 178 (2008) 103–117.
[4] D. Natarajan, T.V. Nguyen, J. Power Sources 115 (2003) 66–80.
[5] C. Song, Y. Tang, J.L. Zhang, J. Zhang, H. Wang, J. Shen, S. McDermid, J. Li, P. Kozak, Electrochim. Acta 52 (2007) 2552–2561.
[6] C.Y. Wang, Chem. Rev. 104 (2004) 4727–4766.
[7] J.T. Gostick, M.W. Fowler, M.A. Ioannidis, M.D. Pritzker, Y.M. Volfkovich, A. Sakars, J. Power Sources 156 (2006) 375–387.
[8] S. Litster, C.R. Buie, T. Fabian, J.K. Eaton, J.G. Santiago, J. Electrochem. Soc. 154 (2007) B1049–B1058.
[9] G. Velayutham, J. Kaushik, N. Rajalakshmi, K.S. Dhathathreyan, Fuel Cells 4 (2007) 314–318.
[10] K. Tüber, D. Pocza, C. Hebling, J. Power Sources 124 (2003) 403–414.
[11] J. Moreira, A.L. Ocampo, P.J. Sebastian, M.A. Smit, M.D. Salazar, P.D. Angel, J.A. Montoya, R. Perez, L. Martinez, Int. J. Hydrogen Energy 28 (2003) 625–627.
[12] G.G. Park, Y.J. Sohn, T.H. Yang, Y.G. Yoon, W.Y. Lee, C.S. Kim, J. Power Sources 131 (2004) 182–187.
[13] D. Bevers, R. Rogers, M.V. Bradke, J. Power Sources 63 (1996) 193–201.
[14] E. Passalacqua, G. Squadrito, F. Lufrano, A. Patti, L. Giorgi, J. Appl. Electrochem. 31 (2001) 449–454.
[15] M. Prasanna, H.Y. Ha, E.A. Cho, S.-A. Hong, I.-H. Oh, J. Power Sources 131 (2004) 147–154.
[16] H.S. Chu, C. Yeh, F. Chen, J. Power Sources 123 (2003) 1–9.
[17] K. Jiao, B. Zhou, J. Power Sources 169 (2007) 296–314.
[18] J. Benziger, J. Nehlsen, D. Blackwell, T. Brennan, J. Itescu, J. Membr. Sci. 261 (2005) 98–106.
[19] H.-J. Butt, K. Graf, M. Kappl, Physics and Chemistry of Interfaces, Wiley-VCH, Weinheim, 2006.
[20] W.G. Gray, C.T. Miller, Environ. Sci. Technol. 38 (2004) 5895–5901.
[21] D.R. Lide, CRC Handbook of Chemistry and Physics, 89th ed., CRC Press, Boca Raton, 2008.
[22] Y.W. Chen-Yang, T.F. Hung, J. Huang, F.L. Yang, J. Power Sources 173 (2007) 183–188.